

On the taxonomy of the genus *Systemostrema* Hazard & Oldacre, 1975 (Microspora, Thelohaniidae), with description of two new species

J.I. Ronny Larsson

Department of Zoology, University of Lund, S-223 62 Lund, Sweden

Accepted for publication 10th March, 1987

Abstract

The paper treats the taxonomy of the genus *Systemostrema* Hazard & Oldacre, 1975, starting with an ultrastructural investigation of two new species, parasitic in larvae of the dragonflies *Aeshna grandis* and *Libellula quadrimaculata*, collected in Sweden. The two species are identical in pathology and presporal stages, but differ in the shape of spores and sporophorous vesicles, the fine structure of the spores, and numerical characters. The new species, which are named *S. alba* and *S. candida*, are compared to the octosporoblastic microsporidia parasitic in Odonata. An emended diagnosis of the genus *Systemostrema* is given, together with a taxonomic summary. The new combinations *S. trichostegiae* for *Thelohania trichostegiae* Baudoin, 1969 and *Amblyospora capillata* for *T. capillata* Larsson, 1983 are established.

Introduction

Hazard & Oldacre (1975) revised the microsporidia close to *Thelohania*, and created the new family Thelohaniidae and eight new genera, including *Systemostrema*. This was the first attempt to make wider use of ultrastructural characters for taxonomy at levels above the species, and the new genera were defined more precisely than previously described microsporidian genera had been. The genus *Systemostrema* was at that time monotypic with the single species *S. tabani*, a parasite of larvae of the horse fly *Tabanus lineola*. Recently, *Thelohania corethrae* Schuberg & Rodriguez, 1915 has been investigated using electron microscopy and found to be a *Systemostrema* species (Larsson, 1986a). No further species have been described in the genus or transferred to it.

An investigation of microsporidia of dragonfly larvae revealed two new *Systemostrema* species, which are described here. Information from four species of the genus gives an opportunity to re-evaluate the diagnostic characters and to emend

the diagnosis for the genus *Systemostrema*. The possible shift of octosporoblastic microsporidia of insects from *Thelohania* to *Systemostrema* is discussed, and the new combination *S. trichostegiae* (Baudoin, 1969) is established.

Materials and methods

Systemostrema alba n. sp. is a parasite of larvae of *Aeshna grandis* (Odonata Aeshnidae) collected in a single pond at Sjödiken, Sweden. The second species, *S. candida* n. sp., was found in larvae of *Libellula quadrimaculata* (Odonata, Libellulidae). This microsporidium is widely distributed in the southern part of Sweden. Material collected at Sandby mosse was selected for the description.

Fresh smears of infected tissue were prepared by the agar method of Hostounský & Žižka (1979) and studied using phase contrast microscopy and dark field illumination. Permanent smears were lightly air-dried and fixed in Bouin-Duboscq-Brasil solution for at least one hour. For paraffin-sectioning

abdominal segments or whole abdomens were fixed in the same fixative overnight or longer, washed and dehydrated in an ascending series of ethanols, and embedded in paraplast. Sections were cut sagittally at 10 µm. Smears and sections were stained using Giemsa solution, Heidenhain's iron haematoxylin, or following a modification of the polychromatic staining by Vetterling & Thompson (1972). The original nuclear staining was substituted with Heidenhain's haematoxylin in an abbreviated procedure: 2.5% (w/v) iron alum solution for one hour, Heidenhain's iron haematoxylin for one hour, and destaining in iron alum solution to desired intensity. After washing in running tap water and distilled water, the procedure recommended by Vetterling & Thompson (1972) was followed from point 4 and onwards. For details on the general histological techniques used see Rommeis (1968). All permanent preparations were mounted in DePeX. Measurements were made with an eye-piece micrometer at $\times 1000$.

For transmission electron microscopy small pieces of infected tissue were excised and fixed in 2.5% (v/v) glutaraldehyde in 0.2 M sodium cacodylate buffer (pH 7.2) at 4°C. Tissues from *Aeshna* larvae were fixed for 27 hours and tissues from *Libellula* larvae for 65 hours. After washing in cacodylate buffer and post fixation in 2% (w/v) osmium tetroxide in cacodylate buffer for one hour at 4°C the pieces were washed and dehydrated in an ascending series of buffer-acetone solutions to absolute acetone, and embedded in epon. Sections were stained with uranyl acetate and lead citrate.

Spores from *Libellula* larvae were smeared on circular cover glasses, lightly air dried and fixed in 2.5% glutaraldehyde in cacodylate buffer at 4°C for 65 hours. After washing in buffer and critical point drying, the smears were covered with metallic gold and palladium and studied using scanning electron microscopy.

Observations

Pathology

Infected *A. grandis* larvae could not be identified from external signs. In opened larvae infection was revealed by a greyish white coloration of the fat body lobes. Larvae of *L. quadrimaculata* with microsporidia were paler than healthy larvae, and the fat body was shining white. In both hosts infection was restricted to the adipose tissue.

The pathology was identical in both hosts. Microsporidia-filled cells appeared in all parts of the lobes, dispersed among unaltered cells (Fig. 1A). Infected fat body cells and their nuclei were hypertrophic, but the infected lobes retained their cellular nature and were not degraded to syncytia.

Presporal stages and life cycle

The two species had similar merogonial and sporogonial stages, and species-specific differences were not apparent until the sporoblast stage.

Merogonial plasmodia of both species were delimited by a c. 7 nm thick unit membrane. The cytoplasm had numerous ribosomes, both free and attached to membranes as a rough endoplasmic reticulum (Fig. 2A). There were also spherical aggregates of vesicles of the type usually interpreted as Golgi apparatuses (Fig. 2A). Nuclei were associated pair-wise as diplokarya, which frequently had electron-dense centriolar plaques at the nuclear periphery (Fig. 2A). Merozoites were lightly oval with a central diplokaryon (Figs 1B, 2B).

In the initial phase of sporogony a thick cover was secreted externally to the plasma membrane (Fig. 2B), and this layer differentiated rapidly into the envelope of the pansporoblast, or preferably the sporophorous vesicle, applying the terminology by Canning & Hazard (1982) (Fig. 3A). The two components of the nuclei moved apart and signs of a meiotic division became visible (Fig. 2C). Synaptonemal complexes appeared as 100–110 nm wide tripartite structures (Fig. 2D). It is of particular interest that in both species synaptonemal polycomplexes, structures not previously reported

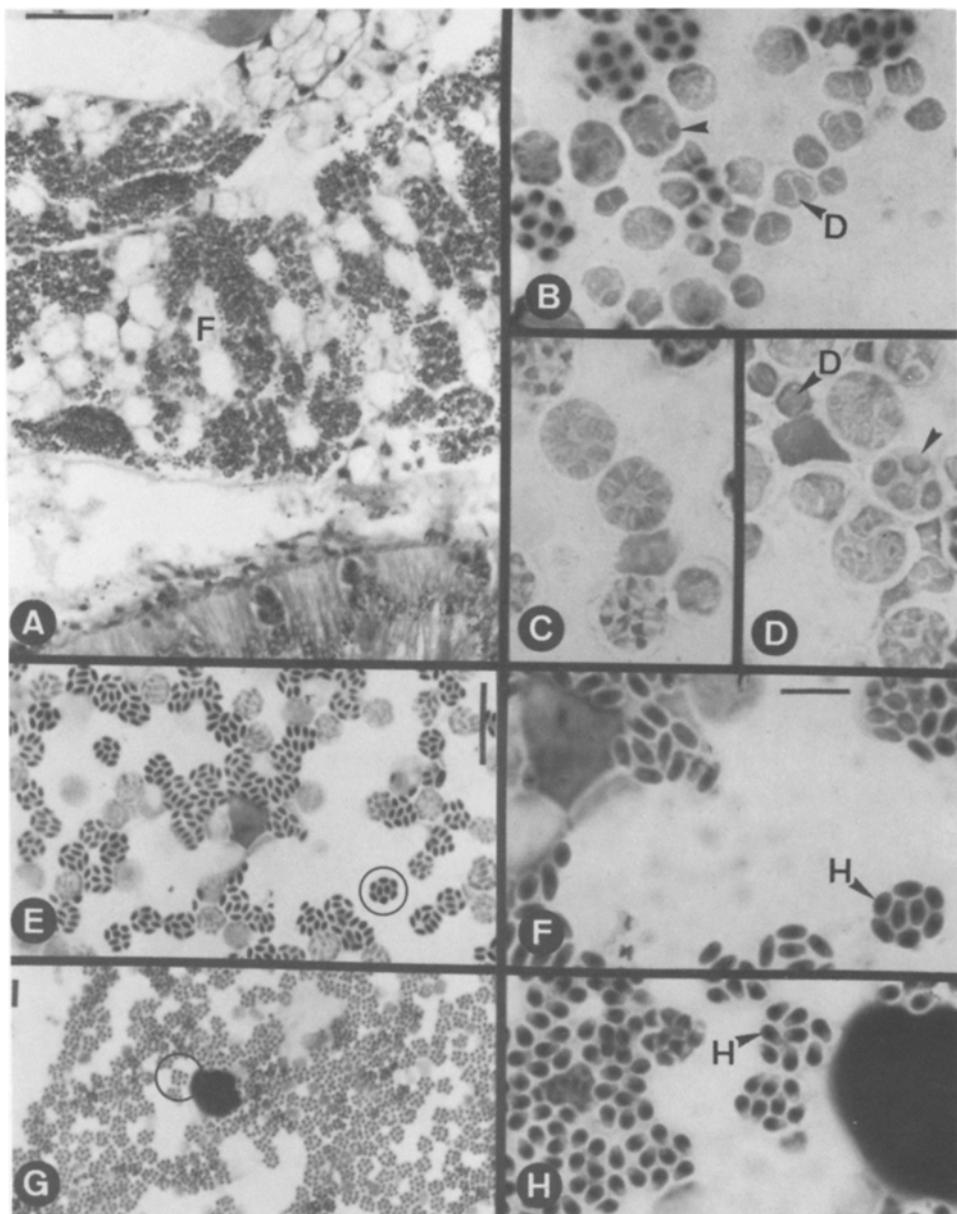


Fig. 1. Light microscopy. Fixed and stained preparations of *Systemostrema alba* n. sp. (C–F) and *S. candida* n. sp. (A–B, G–H). A. Infected fat body with hypertrophic cells; no syncytium is formed. B–D. The end of merogony with diplokaryotic merozoites, and sporogonial plasmodia with four (arrow-head) and eight nuclei. E–F. Localization of the holotype of *S. alba*, slide no. 850821-F-3 RL. G–H. Localization of the holotype of *S. candida*, slide no. 850806-F-1 RL. Abbreviations. D, diplokaryon; F, fat body; H, holotype. A–B & E–H, Heidenhain's haematoxylin; C–D, Giemsa. Scale-bars. A, G. 50 µm; B–D, F, H, with a common bar, 10 µm; E, 10 µm.

from microsporidia, were frequent (Fig. 2E, G). Synaptonemal complexes appeared simultaneously with the first signs of the thick sporont wall. Polycomplexes were typical for sporonts with fully

developed multi-layered cell wall. Ellipsoid, 50–95 nm long structures, similar to recombination nodules were prominent in polycomplexes (Fig. 2G). Approximately 17 nm thick spindle microtu-

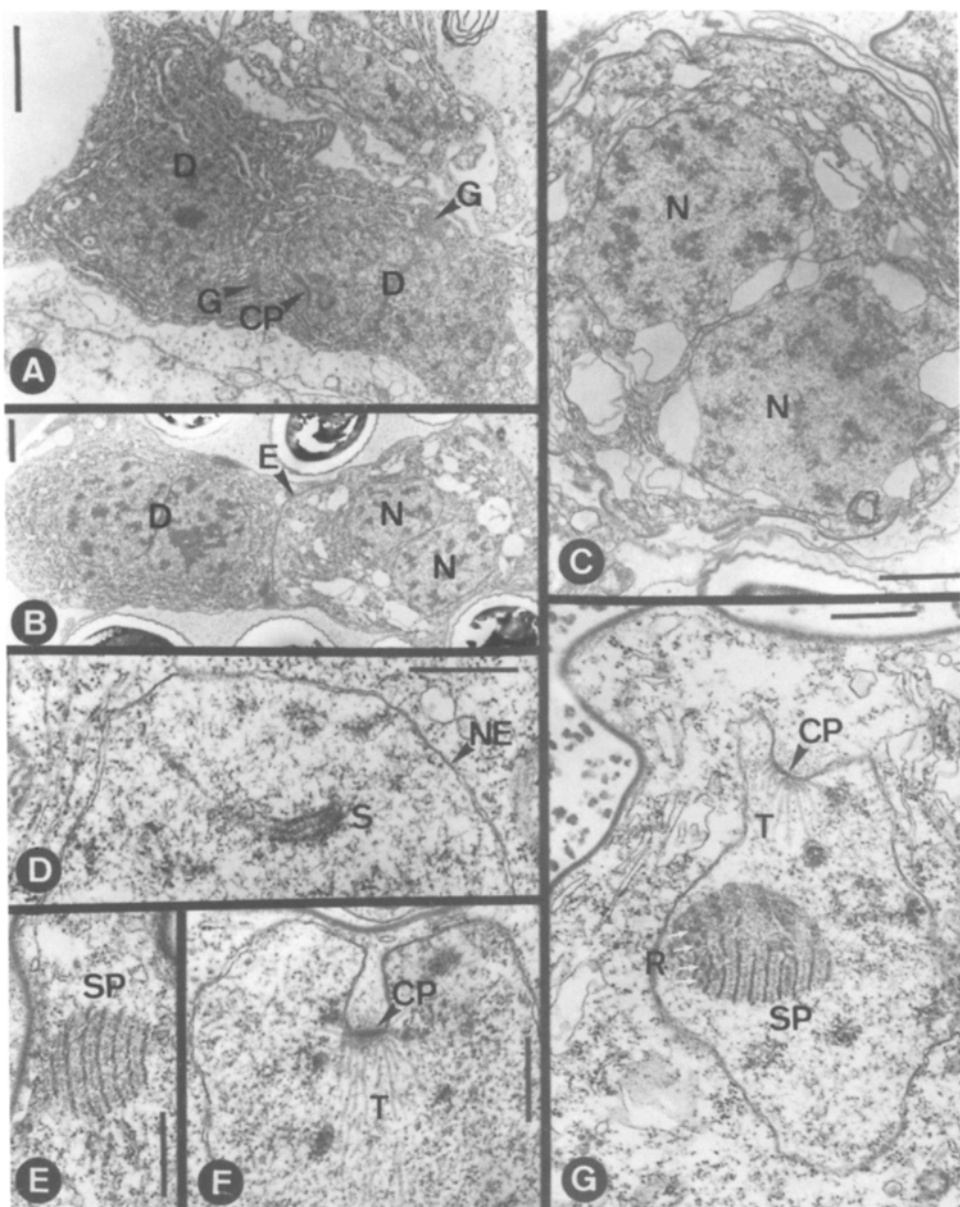


Fig. 2. Electron microscopy. The end of merogony and the meiosis. **A.** Merogonial plasmodium with nuclei arranged as diplokarya. **B.** Two closely associated merozoites; to the left with thin envelope and diplokaryon, to the right in the process of maturation to sporont, with thick envelope and separating nuclei. **C.** Sporont with the two components of the diplokaryon separated; beginning meiosis. **D.** A synaptonemal complex. **E.** A synaptonemal polycomplex. **F.** A deeply invaginated centriolar plaque, with radiating spindle tubules. **G.** Nucleus with indistinct centriolar plaque, radiating tubules, and a synaptonemal polycomplex with equidistant structures resembling recombination nodule-like structures. **A–C, F–G, S. alba n. sp.;** **B–C, E, S. candida n. sp.** Abbreviations. CP, centriolar plaque; D, diplokaryon; E, electron-dense surface layer; G, Golgi apparatus; N, nucleus; NE, nuclear envelope; R, recombination nodule-like structure; S, synaptonemal complex; SP, synaptonemal polycomplex; T, tubule. Scale-bars. **A–C, 1 μm;** **D–G, 0.5 μm.**

bules were organised from invaginated electron-dense centriolar plaques at the nuclear periphery (Fig. 2F–G). The widest well-delimited plaque observed measured 213 nm in diameter.

The sporogonal plasmodia became lobed at the four-nuclei stage (Figs 1D, 3C). Their nuclei divided once more, although the nuclear division was not always perfectly synchronized with the budding of the plasmodium. Usually eight daughter cells (which matured to sporoblasts without further division) were budded off simultaneously. However, in both species it was observed that four daughter cells with dividing nuclei could be released from the plasmodium. These sporoblast mother cells divided once more to produce two sporoblasts each.

The sporoblasts were irregular cells with a central nucleus (Fig. 3D). Their multi-layered cell wall was initiated in the sporont stage. The young sporont of both species produced a c. 10 nm thick uniform layer of moderately electron-dense material externally to the plasma membrane (Fig. 2B). This material lost contact with the sporont and formed blister-like protrusions, the primordia of the sporophorous vesicle (Fig. 3A). A new, 35–38 nm thick, sporont wall was produced from the plasma membrane, inside the blisters, and it developed directly into a three-layered structure, with two moderately electron-dense layers separated by a more dense stratum (Fig. 3A–B). In the sporoblast (Fig. 3D) and the immature spore (Fig. 3E) the cell wall widened successively, in that translucent material was inserted between the plasma membrane and the internal moderately dense layer. In the sporoblast the dense, uniform median stratum was split to a double-layer, resembling a unit membrane (Fig. 3D, inset), which persisted unchanged in immature (Fig. 3E) and mature spores (Figs 5C, 6C).

The characteristic organelles developed, associated with cytoplasmic vesicles, in the way usual for microsporidia. The polar sac, inside which the anchoring apparatus was formed, originated close to the nucleus (Fig. 3D). Material was incorporated to a growing polar filament, the polar sac was pushed to the anterior pole, and the coiled filament was stored in the posterior half of the immature spore (Fig. 3E). At this stage the vesicles generat-

ing the filament were associated to a voluminous, spongy structure (Fig. 3E), the posterosome using the terminology by Weiser & Žižka (1975), which is a regular component of the immature microsporidian spore, interpreted as a Golgi apparatus. Later the polar sac and filament were covered with a unit membrane (Fig. 3F), and the anchoring disc originated as a bowl-shaped body in the polar sac (Fig. 3F).

The sporophorous vesicle, initiated as protrusions from the sporont, was delimited by a c. 10 nm thick envelope of uniform electron-dense material (Fig. 3A). The episporontal space, using the terminology by Vávra (1984), initially contained amorphous aggregates of electron-dense material, apparently projections from the wall of the sporont (Fig. 3A). This material was organised into tubules with walls of identical construction to that of the sporont wall (Fig. 4C). During the sporoblastogenesis the walls of the tubules were modified in an identical way to the wall of the sporogonial plasmodium, in that new material was inserted between the plasma membrane and the double-layer. In young vesicles tubules were more or less regularly arranged, often in strands in parallel with the wall of the sporogonial plasmodium (Fig. 4D). The internal cavity of the tubules, lined by unit membranes, was originally a continuous, undivided space (Fig. 4E). In sporophorous vesicles with mature spores, the central cavity of the persistent tubules was split into spherical or oval compartments at approximately equal distances (Fig. 4F). Tubules of vesicles with mature spores were 80–85 nm wide, the diameter of the central cavity was 27–32 nm, identically in both microsporidia.

The two species differed in shape and dimensions of the sporophorous vesicles. Vesicles of *S. alba* were almost perfectly spherical (Fig. 4A), with a uniform diameter of c. 11 µm. Vesicles of *S. candida* were more or less ellipsoid, c. 8 × 10.8 µm wide (Fig. 4B).

The mature spores

Mature spores of the two species differed prominently both in shape and in numerical characters,

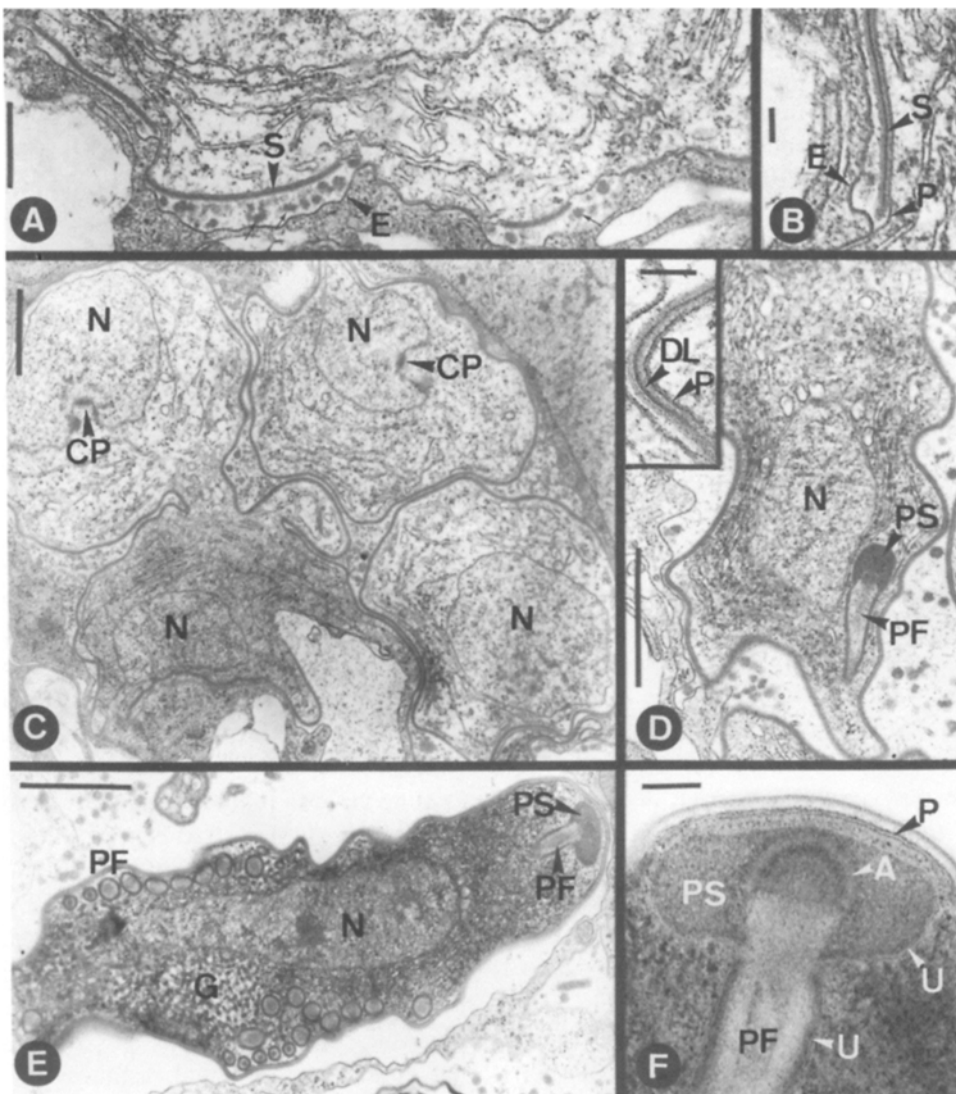


Fig. 3. Electron microscopy. The sporoblastogenesis and the morphogenesis of the spore. **A.** The periphery of a sporogonial plasmodium, with the envelope of the sporophorous vesicle initiated as blister-like protrusions of electron-dense material; black arrows indicate the amorphous aggregates of electron-dense material in the episporontal space. **B.** The thick wall of the sporogonial plasmodium is secreted from the plasmodium, inside the primordia of the sporophorous vesicle. **C.** Lobed sporogonial plasmodium in the four-nuclei stage (cf. Fig. 2D); the isolated nuclei are dividing. **D.** Sporoblast with the first signs of the polar sac and the polar filament; inserted detail shows the development of the double-layer of the exospore. **E.** The immature spore. **G.** Anterior end of an immature spore with the first signs of the anchoring disc. **A–E,** *S. alba* n. sp.; **F,** *S. candida* n. sp. Abbreviations. **A**, anchoring disc; **CP**, centriolar plaque; **DL**, double-layer; **E**, envelope of the sporophorous vesicle; **G**, Golgi apparatus (posterosome); **N**, nucleus; **P**, plasma membrane; **PF**, polar filament; **PS**, polar sac; **S**, developing thick wall of the sporogonial plasmodium; **U**, unit membrane. Scale-bars. **A**, 0.5 μ m; **B**, **D**, **F**, 100 nm; **C**, **E**, 1 μ m.

and the spores are therefore treated separately for each species.

Systemostrema alba n. sp.

Mature spores were ovoid to lightly pyriform with a blunt anterior pole (Figs 1F, 5A). Unfixed spores measured $2.5\text{--}3.0 \times 4.9\text{--}6.3 \mu\text{m}$, fixed and stained

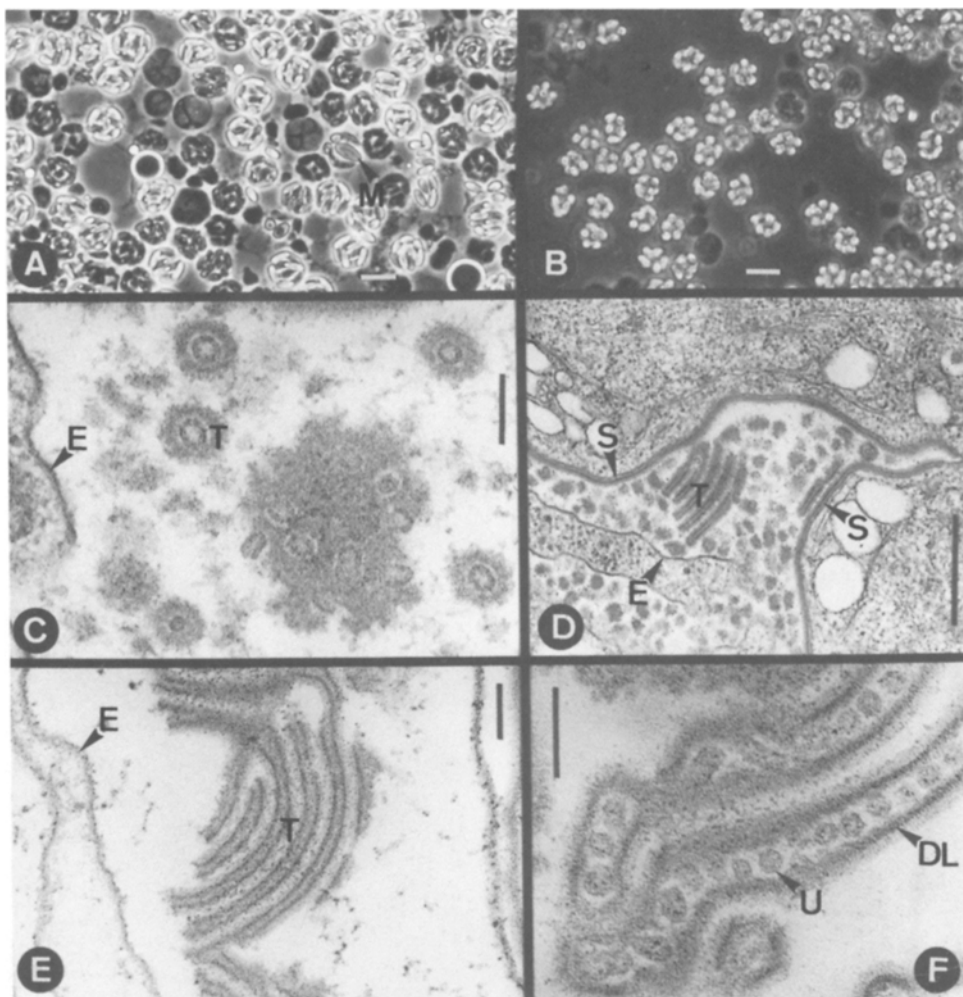


Fig. 4. A–B, light microscopy; C–F, electron microscopy. The sporophorous vesicle. A. Unfixed spherical sporophorous vesicles of *S. alba* n. sp.; one macrospore visible. B. Unfixed oval-rounded sporophorous vesicles of *S. candida* n. sp. C–D. Episporontal space with tubular inclusions, exhibiting layers similar to those of the wall of the sporogonial plasmodium, the unit membrane lining of the central cavity is derived from the plasma membrane; the tubules are sometimes regularly arranged, often lying parallel with the wall of the plasmodium. E. Tubules with a continuous internal cavity in vesicles with immature stages. F. Tubules of vesicles with mature spores; the central cavity is split into serially arranged compartments. A, C–D, *S. alba* n. sp.; B, E–F, *S. candida* n. sp. Abbreviations. DL, double-layer; E, envelope of the sporophorous vesicle; M, macrospore; S, wall of the sporogonial plasmodium; T, tubule; U, unit membrane. Scale-bars. A–B, 10 µm; C, E–F, 100 nm; D, 0.5 µm.

spores $1.8\text{--}2.2 \times 3.0\text{--}4.8 \mu\text{m}$. Macrospores (Fig. 4A) were fairly common, the largest observed measured unfixed $4.1 \mu\text{m}$ wide and $9.0 \mu\text{m}$ long.

The spore wall was 213–275 nm thick (considerably thinner, c. 70 nm, above the anchoring apparatus): with a c. 7 nm thick plasma membrane, a wide translucent endospore, and a c. 27 nm thick stratified exospore, which had a moderately elec-

tron-dense internal layer of approximately uniform thickness, a. c. 5 nm wide double-layer, the most dense and prominent layer of the spore wall, and a surface layer externally and internally delimited by more translucent material (Fig. 5C).

The polar filament had a short straight part, c. 1/8 of the spore length, an oblique section and one layer of coils (Fig. 5B). The coiled part began about

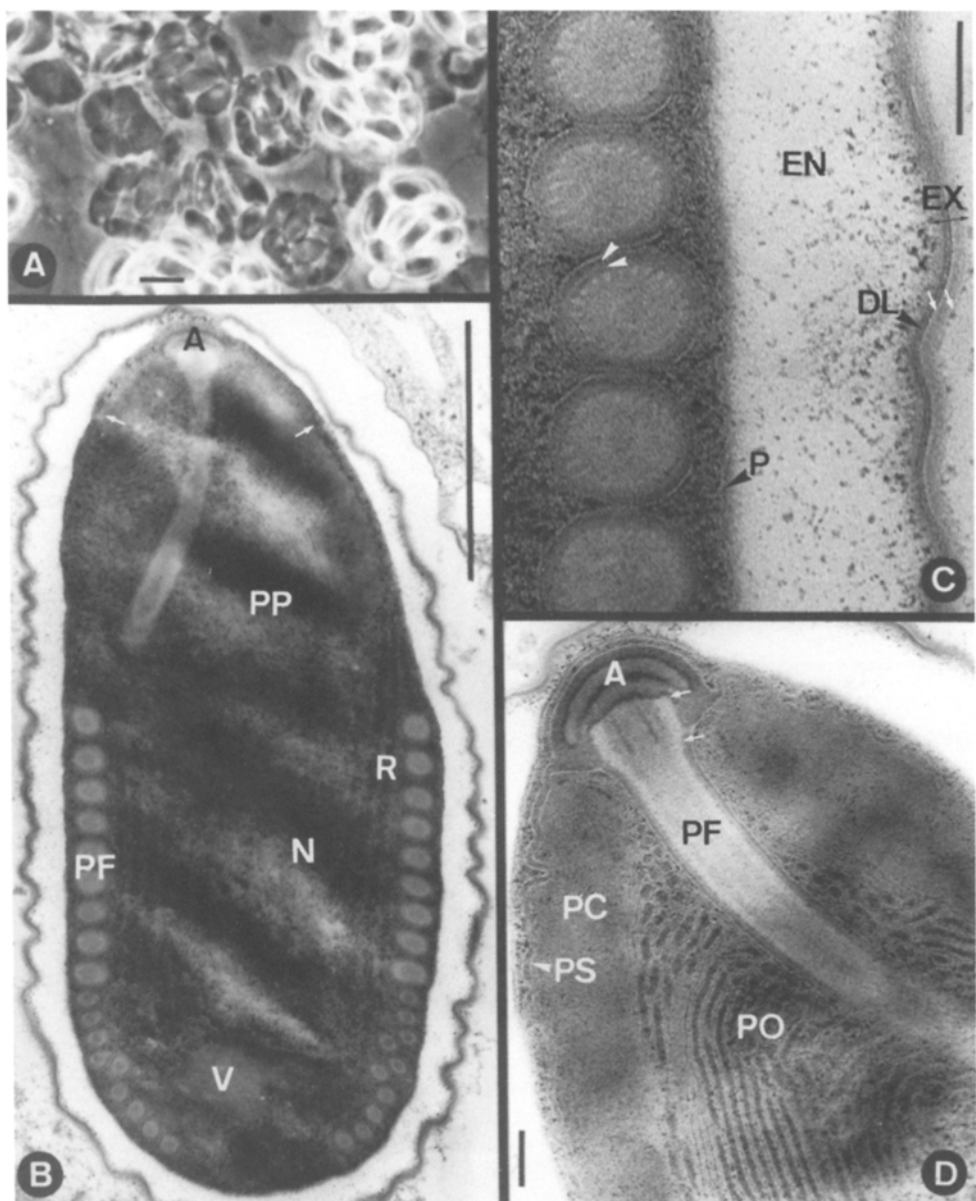


Fig. 5. The mature spore of *S. alba* n. sp. (A, light microscopy; B–D, electron microscopy). A. Unfixed spores in sporophorous vesicles. B. Longitudinally sectioned spore; white arrows indicate the extensions of the polar sac. C. Spore wall and transversely sectioned polar filament coils; white arrows indicate the more translucent external and internal lining of the surface layer of the exospore; white arrow-heads indicate the two layers of different electron density internal to the unit membrane of the polar filament. D. Anterior end of a spore, showing the organisation of the polaroplast and the anchoring apparatus of the polar filament; white arrows show the extension of the wide attachment section. Abbreviations. A, anchoring disc; DL, double-layer; EN, endospore; EX, exospore; N, nucleus; P, plasma membrane; PC, cavum-like part of the polaroplast; PF, polar filament; PO, posterior part of the polaroplast; PP, polaroplast; PS, polar sac; R, ribosomes; V, posterior vacuole. Scale-bars. A, 5 µm; B, 1 µm; C–D, 100 nm.

2/5 from the anterior pole of the spore. The angle of tilt of the anterior filament coil to the long axis of the spore was c. 55°. The polar filament was anisofilar with 9–11, 122–144 nm wide, anterior coils, and 9–10, 89–96 nm wide, posterior coils. The section with wide coils ended approximately 1/4 from the posterior pole of the spore. In the polar sac the filament widened to a short attachment section (Fig. 5D). The curved anchoring disc, with a maximum diameter of 239 nm, had externally a layer of stratified electron-dense material (Fig. 5D), resembling a unit membrane, but considerably thinner. The transversely sectioned filament (Fig. 5C) had an external unit membrane lining and half-way to the centre an electron-lucent layer, resembling fibrils or a ring with pointed interior projections. Between these layers were two equally thick zones, the outermost one was the most electron-dense layer of the filament. The wide centre was moderately electron-dense, with an internal zone of more translucent material.

The polaroplast had two lamellar parts (Fig. 5B, D). The anterior lamellae were very closely packed, with a periodicity of c. 5 nm, resembling a cavum, using the terminology by Sprague, Vernick & Lloyd (1968) (Fig. 5D). The cavum-like part occupied approximately 1/5 of the total length of the polaroplast, and it surrounded the front end of the posterior lamellae in a cap-like manner. The posterior c. 21 nm wide lamellae were also regularly arranged (Fig. 5D). The polaroplast tapered successively and ended at the anterior filament coil, slightly below the middle of the spore. The posteriorly directed extensions of the polar sac were c. 20 nm thick, enclosing approximately half the cavum-like part of the polaroplast (Fig. 5B).

The elongate nucleus was localized to the posterior half of the spore (Fig. 5B). The largest measured sectioned nucleus was 1.3 µm in diameter. The membrane-lined posterior vacuole was fairly small, the widest seen measured 70 nm in diameter. It was located in the mid-line of the spore close to the posterior tip (Fig. 5B). The granular cytoplasm had prominent strands of membrane-lined ribosomes.

Systemostrema candida n. sp.

Mature spores had distinct pyriform shape (Figs 1H, 6A–B). They had fairly uniform dimensions: unfixed they measured 3.2–3.5 × 5.1–5.6 µm, fixed and stained 2.2–2.8 × 3.5–4.4 µm. Macrospores were not observed.

The spore wall was 195–293 nm thick (as thin as 55 nm above the anchoring apparatus): with a c. 7 nm thick plasma membrane, a wide structureless endospore, and a stratified exospore, c. 28 nm thick, with an internal moderately dense layer, an electron-dense c. 5 nm thick double-layer, and a moderately dense surface layer, with more translucent external and internal linings (Fig. 6C).

The polar filament had anteriorly a short straight part, c. 1/10 of the spore length, and an oblique section leading to the coiled part, beginning about 1/4 from the anterior pole of the spore (Fig. 6E). The angle of tilt was 55–60°. The coils were arranged in one layer. The filament was anisofilar with 9–11, 144–186 nm wide, coils anteriorly, 4–5, 71–78 nm wide, coils posteriorly. The section with wide coils almost touched the posterior pole of the spore. The attachment section of the filament was slightly broader than the filament proper and very short, enclosed by the polar sac (Fig. 6F). The widest curved anchoring disc measured was 277 nm in diameter. The transversely sectioned filament (Fig. 6D) had an identical stratification to the filament of the previous species.

The polaroplast had two lamellar parts. The cavum-like anterior part was very short, less than 1/10 of the polaroplast length (Fig. 6F). The anterior lamellae were tightly compressed, with a periodicity of less than 5 nm. The c. 20 nm wide posterior lamellae were regularly arranged. The posterior end of the polaroplast tapered to a position slightly below the first wide filament coil, approximately 1/3 from the posterior end of the spore (Fig. 6E). The posteriorly directed part of the polar sac was c. 15 nm wide, and enclosed almost completely the cavum-like polaroplast (Fig. 6E).

The elongate nucleus (the widest diameter measured in sections was 1.3 µm) was inserted obliquely between the polaroplast and a big, almost lateral posterior vacuole, usually more than 1 µm in diameter (Fig. 6E). Strands of membrane-bound ribosomes were prominent in the granular cytoplasm.

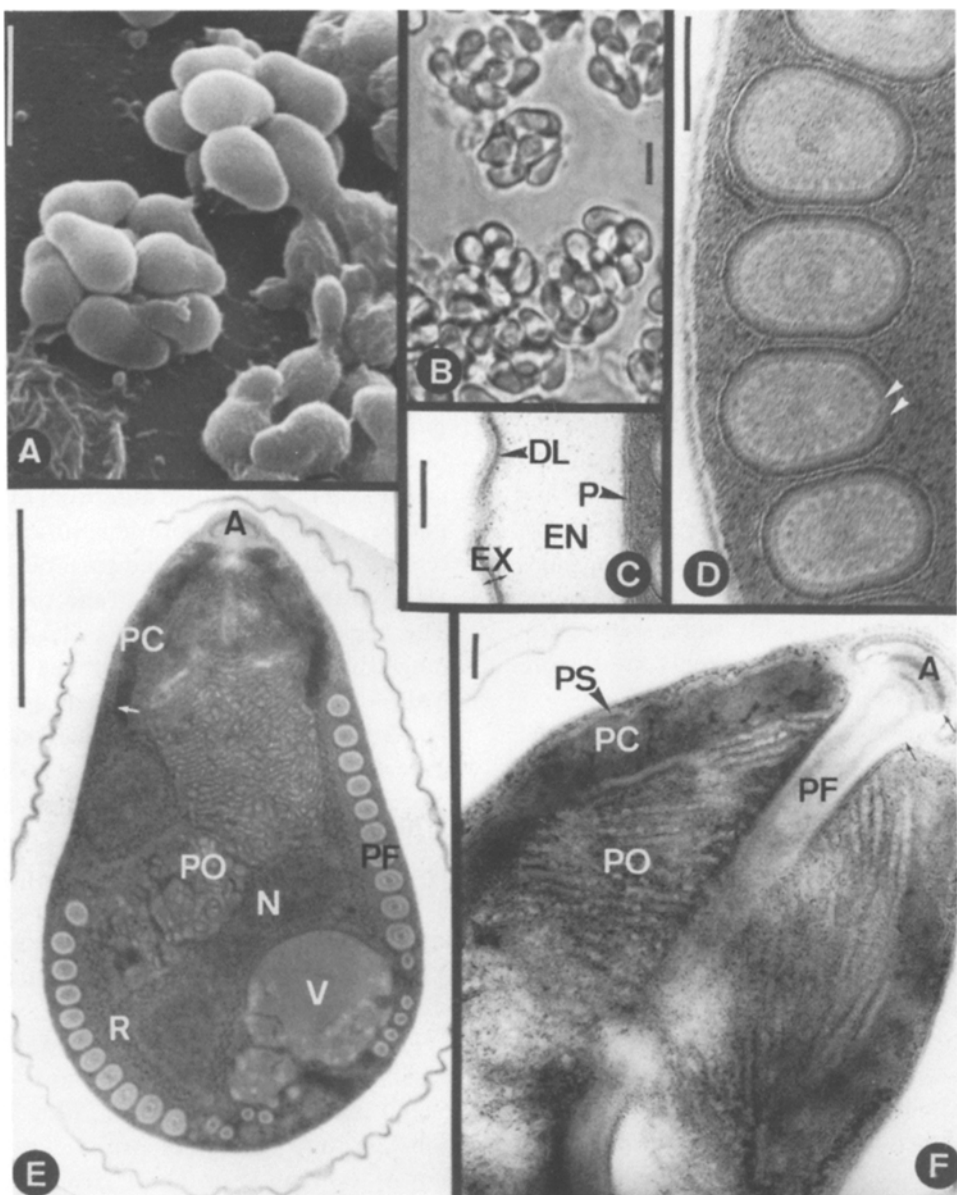


Fig. 6. The mature spore of *S. candida* n. sp. (A, scanning electron microscopy; B, light microscopy; C–F, transmission electron microscopy). A. Sporophorous vesicles with spores. B. Unfixed vesicles with spores. C. The spore wall. D. Transversely sectioned wide polar filament coils; white arrow-heads indicate the layers immediately internal to the unit membrane. E. Longitudinally sectioned spore; white arrow shows the extension of the polar sac. F. Anterior end of the spore, showing the organisation of the polaroplast and the anchoring apparatus of the polar filament; black arrows indicate the extension of the wide attachment section. Abbreviations. A, anchoring disc; DL, double-layer; EN, endospore; EX, exospore; N, nucleus; P, plasma membrane; PC, cavum-like part of the polaroplast; PF, polar filament; PO, posterior part of the polaroplast; PS, polar sac; V, posterior vacuole. Scale-bars. A–B, 5 µm; C–D, F, 100 nm; E, 1 µm.

Discussion

Morphology and reproduction

The morphology, morphogenesis of the organelles and modes of reproduction were identical to what was previously known about microsporidia of the Thelohaniidae, and they need no special comments. The only unusual thing observed was the structures identified as synaptonemal polycomplexes. Such structures, which look like closely assembled synaptonemal complexes (Fig. 2E, G) are previously known to occur both in animals, like the nematode *Ascaris suum* (see Bogdanov, 1977) and grasshoppers (Esponda & Krimer, 1979) and in plants like *Paeonia* and *Tradescantia* species (Kehlhoffner & Dietrich, 1983). Most observations are from insects. To my knowledge, however, there is only one previous observation from protozoa: the ciliate *Dileptus anser* (see Vinnikova, 1976). The function of the synaptonemal polycomplexes is still an enigma, but they have been suggested to represent transient storage sites of synaptonemal complex material (Fil, Goldstein & Moens, 1977). It is also unclear if they are composed of reassembled material of synaptonemal complexes or if they are newly formed structures. Esponda & Krimer (1979) and Fuge (1979) suggested that the synaptonemal complexes disintegrated during late diplotene and the units were stacked during the first metaphase, forming the polycomplexes. In both microsporidia investigated here the synaptonemal complexes preceded the polycomplexes (the age of the sporont was revealed not only by the meiotic configuration, but also from the degree of development of the continuously growing complex cell wall), which might support the hypothesis that polycomplexes are formed by reassembled synaptonemal complex units.

Microsporidia of the Odonata

Eight species of microsporidia have been described from larvae of dragonflies. Three of them have octosporous sporogony in sporophorous vesicles and probably belong in the family Thelohaniidae.

Two species have rod-shaped spores: *Toxoglugea tillargi*, described by Kalavati & Narasimhamurti (1978), and *Resiomeria odonatae*, described by Larsson (1986b). These differ in spore shape from the species treated here. The third species, *Thelohania limbata*, described by Narasimhamurti, Naazier Ahamed & Kalavati (1980), has oval spores, $3.6 \times 7.2 \mu\text{m}$, with one nucleus and a large posterior vacuole. The sporophorous vesicles are $13.2 \times 14.4 \mu\text{m}$. All measurements were probably made on fixed and stained preparations. The microsporidium is a parasite of *Tramea limbata* in India, developing in the adipose tissue. The pathology is characteristic, in that conspicuous, 1.0–1.5 mm wide, cysts are formed around several sporophorous vesicles.

Thelohania limbata has only been studied using light microscopy, and the identification of the genus was made tentatively from the octosporous sporogony. It could equally well be a *Systemostrema* species, but the question about the genus can only be answered by an ultrastructural investigation. However, *T. limbata* is different from the two microsporidia of dragonflies treated here. *Systemostrema candida* has different spore shape and smaller spores. Spores of *T. limbata* resemble spores of *S. alba*, but they are intermediate in size to micro- and macrospores of *S. alba*. Macrospores were not reported from *T. limbata*. Also the histopathology is different, in that no cysts are formed around sporophorous vesicles of *S. alba*.

The genus Systemostrema

Agmasoma, *Hyalinocysta* and *Systemostrema*, three of the new genera described by Hazard & Oldacre (1975) share some important taxonomic characters with *Thelohania*. All have pyriform spores, identical stratified exospores of approximately the same thickness (with some uncertainty about *Hyalinocysta*) and sporophorous vesicles devoid of amorphous or crystalline aggregates of the type characteristic for the genera *Amblyospora*, *Chapmanium*, *Cryptosporina* and *Parathelohania*.

The type-species of *Thelohania*, *T. giardi* Henne-guy, 1892, has not been investigated by modern

techniques, and the ultrastructural cytology is unknown. The present conception of the genus is based on ultrastructurally investigated microsporidia of decapod crustaceans, presumed to be congeneric with the type-species. The genus *Thelohania* is currently distinguished from *Agmasoma*, *Hyalinocysta* and *Systemostrema* by having an isofilar polar filament, while the filament of the other three genera is anisofilar.

Hazard & Oldacre (1975) considered *Agmasoma* so different from the other *Thelohania*-like microsporidia that the genus probably should be placed in a family of its own. The sporoblasts are not formed by the cytoplasmic budding typical for the other genera. No publications dealing with this genus have appeared since the description.

Hyalinocysta, like *Agmasoma* and *Systemostrema*, was described on the investigation of a single species. *Hyalinocysta* and *Systemostrema* are morphologically very similar, the only difference being that the sporophorous vesicle of *H. chapmani* is completely devoid of inclusions, while the vesicle of *S. tabani* has tubular inclusions. Even though the diagnosis of the genus *Hyalinocysta* was based on an ultrastructural investigation of the type species, there are still outstanding questions about its cytology, and it is possible that new investigations might reveal unique characters. Until it has been proven that there are no further differences between the genera, both should be considered valid.

There is one important lacuna in the description of *S. tabani*. The polaroplast was not correctly preserved in the material used for the description, and it is not clear that the species has a polaroplast with two lamellar parts.

The two species of dragonfly larvae treated here agree in all comparable characters with the type-species of *Systemostrema*. In addition, *Thelohania corethrae* Schuberg & Rodriguez, 1915, has been investigated using electron microscopy and found to accord with the characteristics of the type-species of *Systemostrema* (Larsson, 1986a). A summary of the characteristics of the type-species and the three other species permits an amended diagnosis for the genus *Systemostrema*.

In the revision Hazard & Oldacre (1975) treated

Thelohania as a genus parasitic in decapod crustaceans, and listed a number of doubtful *Thelohania* species. Numerous *Thelohania* species have been reported from insects, and with few exceptions the identification of the genus has been based solely on the octosporous sporogony. A few of these species have light microscopic characters which suggest a new generic affiliation, and some of them have been transferred to *Amblyospora*, *Parathelohania* or *Chapmanium*. Most of the old *Thelohania* species remain in the genus, waiting for new investigations to solve the taxonomic problems. Probably a number of these *Thelohania* species actually belong in *Systemostrema*. However, the genus *Thelohania* is not unique to crustaceans. There are octosporoblastic microsporidia of insects, which have an isofilar polar filament and also agree with the other characters of *Thelohania*, including the exospore. Such microsporidia are for example present in midge larvae in Sweden (Larsson, unpublished), and it is obvious that we cannot directly transfer all *Thelohania* species of insects, which have pyriform spores and rounded sporophorous vesicles, to *Systemostrema*. The insect parasite *Thelohania capillata* was assigned to *Thelohania* solely by the presence of a uniformly thick polar filament (Larsson, 1983), as this character was considered especially important in the revision by Hazard & Oldacre (1975). However, today we know more about the microsporidia of Thelohaniidae and Amblyosporidae, and it is clear that the barrel-shaped spores and the thick, lamellar basal layer of the exospore are characters unique to octospores of *Amblyospora* species. These characters are present in *T. capillata*, together with the amorphous inclusions of the episporontal space, which are regularly seen in *Amblyospora* species. Consequently the uniform polar filament of *T. capillata* must be interpreted as a reduced anisofilar filament, where the narrow distal part has disappeared, not as an isofilar filament. The reduced filament and the characteristic envelope of the sporophorous vesicle make *Amblyospora capillata* n. comb. still a valid species.

Baudoin (1969) described three new microsporidian parasites of Trichoptera. Two of the species were identified as belonging in *Thelohania*. Both were illustrated by electron micrographs. One of

the species, *T. bicortex*, is a clear *Amblyospora* species, and it was transferred to that genus by Hazard & Oldacre (1975). They also transferred the second species, *T. trichostegiae*, to *Amblyospora*, interpreting the spores described as belonging to a free, diplokaryotic spore line of a dimorphic species in females. However, this action was caused by an erroneous interpretation of the description. Hazard & Oldacre (1975) stated about the spores '... nor does he mention if they are bound in groups of eight in a pansporoblastic membrane ...', and '... The spore appears to be binucleate ...'. Baudoin (1969) stated very clearly in the description '... Il a été possible d'observer des pansporoblastes, de 15 µm de diamètre, à l'intérieur desquels les spores sont groupées par 8, légitimant l'appartenance de l'espèce au genre *Thelohania* ...', and in the description of the mature spore is written '... Cette partie basale contient le noyau ...'. There is no ground for considering these spores as belonging to a free diplokaryotic cycle, and an affiliation in *Amblyospora* is excluded.

Even if not all important taxonomic characters are visible in the micrographs by Baudoin (1969), the spore shape, the fine structure of the polar filament, the tubular inclusions of the sporophorous vesicle, and probably also the polaroplast agree with the cytology of *Systemostrema*. A longitudinally sectioned mature spore shows a polar filament, where an anterior series of coils forms a distinct layer close to the spore wall, while a posterior irregular group of coils is pushed to the interior of the spore. The regularly arranged anterior coils have a more translucent median layer than the posterior ones. The quality of the micrograph is not sufficiently good to measure individual coils, but the diameter of the anterior coils is apparently slightly wider than the diameter of the posterior ones. The arrangement of coils in two distinct groups, the structural difference between anterior and posterior coils, and the fairly clear differences in width indicate that it is an anisofilar polar filament. If we add characters like the spore shape, the monokaryotic spore, the tubular inclusions of the sporophorous vesicle, and the insect host, we have a fairly good base for transferring the species to the genus *Systemostrema*.

Taxonomic summary and descriptions

Hazard & Oldacre (1975) gave the following characteristics for the new genus *Systemostrema*: One developmental sequence known, which produces octospores. Pansporoblasts spherical to subspherical, octospores oval-pyriform. Pansporoblastic membrane subpersistent. Octospore has thin exospore, one long polar filament abruptly constricted near its middle, and one indistinct polaroplast. Surface of spore covered with fine ridges, making it somewhat wrinkled. Dividing sporonts secrete granules of uniform size within pansporoblastic membrane, which are mostly replaced by microtubules during sporulation.

The authors remarked that the indistinct polaroplast might be a result of improper spore fixation. The wrinkled surface is a common artifact in spores with fairly thin exospores, and also seen in the sectioned spores of both species investigated here (Figs 5B, 6E). The SEM-picture of *S. candida* (Fig. 6A) shows that the spore wall actually is smooth. The granules of the episporontal space of *S. tabani* (Fig. 83, Hazard & Oldacre, 1975) are identical to the amorphous or fibrillar material seen in the micrograph of *S. alba* (Fig. 3C). The spores of *S. tabani* have the same pyriform shape as spores of *S. candida* (Figs 1H, 6A). The diagnosis for *Systemostrema* is amended in the following way:

Genus *Systemostrema* Hazard & Oldacre, 1975

Merogony diplokaryotic. Merogonial plasmodium divides into numerous merozoites. Diplokaryotic sporont divides meiotically. Eight monokaryotic sporoblasts usually bud off simultaneously from eight-lobed plasmodium. Spores pyriform. Polaroplast with two regularly arranged lamellar parts: narrow and closely arranged lamellae anteriorly, and widely spaced lamellae posteriorly. Exospore layered, with uniform internal stratum, distinct c. 5 nm thick double-layer, and external uniform part with more translucent external and internal linings (Fig. 5C). Polar filament anisofilar. Sporophorous vesicle spherical or lightly oval. Envelope thin and uniform, more or less persistent. Episporontal

space in newly formed vesicles with amorphous or fibrillar inclusions. Older vesicles with thick-walled tubules, exhibiting layers similar to those of exospore. Episporontal space always devoid of granular or crystal-like inclusions. Only one sporogonial sequence observed.

Species

1. *S. tabani* Hazard & Oldacre, 1975, type-species.

2. *S. alba* n. sp.

Spores. Elongate pyriform. Dimensions: unfixed $2.5\text{--}3.0 \times 4.9\text{--}6.3 \mu\text{m}$; fixed and stained $1.8\text{--}2.2 \times 3.0\text{--}4.8 \mu\text{m}$. Macrospores, greatest dimensions $4.1 \times 9.0 \mu\text{m}$ (unfixed), not unusual. Spore wall 213–275 nm thick, exospore c. 27 nm. Polar filament with 9–11, 122–144 nm wide, coils anteriorly, 9–10, 89–96 nm wide, coils posteriorly, in single layer close to spore wall. Coiled part begins approximately 2/5 from anterior pole, and wide coils end approximately 1/4 from posterior pole of spore. Angle of tilt of the anterior coil c. 55°. Anterior polaroplast lamellae occupy approximately 1/5 of polaroplast length. Polar sac encloses anterior half of anterior polaroplast region. Posterior vacuole small, central, close to posterior pole of spore.

Sporophorous vesicle. Regular spherical shape, dimension fairly constant c. $11 \mu\text{m}$ in diameter (unfixed).

Type-host. *Aeshna grandis* (Linnaeus, 1758) (Odonata, Aeshnidae), larvae.

Type-locality. A pond at Sjödiken, Scania, Sweden.

Type-material. Holotype (Fig. 1E–F) on slide no. 850821-F-3 RL, paratypes on slides no. 850821-F-(1-133) RL.

Etymology. The name alludes to the greyish white colour of infected tissue.

Deposition of types. As for *S. candida* n. sp.

3. *S. candida* n. sp.

Spores. Broadly pyriform. Dimensions: unfixed $3.2\text{--}3.5 \times 5.1\text{--}5.6 \mu\text{m}$; fixed and stained $2.2\text{--}2.8 \times 3.5\text{--}4.4 \mu\text{m}$. Spore wall 195–293 nm thick,

exospore c. 28 nm. Polar filament with 9–11, 144–186 nm wide, coils anteriorly, 4–5, 71–78 nm wide, coils posteriorly, in single layer close to spore wall. Coiled part begins approximately 1/4 from anterior pole, and wide coils usually touch posterior pole. Angle of tilt of the anterior coil 55–60°. Anterior part of polaroplast less than 1/10 of total polaroplast length. Total length of polaroplast more than half of spore length. Polar sac encloses nearly completely anterior part of polaroplast. Posterior vacuole large, in lateral position.

Sporophorous vesicle. Spherical to lightly oval, 8– $10.8 \mu\text{m}$ in diameter (unfixed).

Type-host. *Libellula quadrimaculata* Linnaeus, 1758 (Odonata, Libellulidae), larvae.

Type-locality. A pond at Sandby mosse, Scania, Sweden.

Type-material. Holotype (Fig. 1G–H) on slide no. 850806-F-1 RL, paratypes on slides no. 850806-F-(1-99) RL.

Etymology. The name alludes to the shining white colour of infected tissue.

Deposition of types. The slides with the holotypes in the International Protozoan Type Slide Collection, Smithsonian Institution, Washington, D.C., U.S.A. Paratypes in the collection of Dr. J. Weisser, Prague, Czechoslovakia, and in the collection of the author.

4. *S. corethrae* (Schuberg & Rodriguez, 1915) Larsson, 1986.

Synonyms. *Thelohania corethrae* Schuberg & Rodriguez, 1915; *Plistophora chaobori* Rapsch, 1950.

5. *S. trichostegiae* (Baudoin, 1969) n. comb.

Synonyms. *Thelohania trichostegiae* Baudoin, 1969; *Amblyospora trichostegiae* (Baudoin, 1969) Hazard & Oldacre, 1975.

Acknowledgements

The author is greatly indebted to Mrs. Lina Hansén, Mrs. Inga Jogby, Mrs. Inger Norling and Mrs. Inga-Lill Palmquist, all at the Department of Zoology, University of Lund, for skilful technical assistance, and to Dr. Ulf Norling, Dept. of Zoology,

Lund, for the identification of the dragonfly larvae. The investigation was financially supported by grants from the Swedish Natural Science Research Council.

References

- Baudoin, J. (1969) Nouvelles espèces de Microsporidies chez des larves de Trichoptères. *Protistologica*, **5**, 441–446.
- Bogdanov, Y.F. (1977) Formation of cytoplasmic synaptonemal-like polycomplexes at leptotene and normal synaptonemal complexes at zygotene in *Ascaris suum* male meiosis. *Chromosoma*, **61**, 1–21.
- Canning, E.U. & Hazard, E.I. (1982) Genus *Pleistophora* Gurley, 1893: an assemblage of at least three genera. *Journal of Protozoology*, **29**, 39–49.
- Esponda, P. & Krimer, D.B. (1979) Development of the synaptonemal complex and polycomplex formation in three species of grasshoppers. *Chromosoma*, **73**, 237–245.
- Filil, A., Goldstein, P. & Moens, P.B. (1977) Precocious formation of synaptonemal-like polycomplexes and their subsequent fate in female *Ascaris lumbricoides* var. *suum*. *Chromosoma*, **65**, 21–35.
- Fuge, H. (1979) Synapsis, desynapsis, and formation of polycomplex-like aggregates in male meiosis of *Pales ferruginea* (Diptera, Tipulidae). *Chromosoma*, **70**, 353–373.
- Hazard, E.I. & Oldacre, S.W. (1975) Revision of microsporidia (Protozoa) close to *Thelohania*, with descriptions of one new family, eight new genera, and thirteen new species. *Technical Bulletin United States Department of Agriculture*, no. 1530, 1–104.
- Hostounský, Z. & Žižka, Z. (1979) A modification of the 'agar cushion method' for observation and recording microsporidian spores. *Journal of Protozoology*, **26**, 41A–42A.
- Kalavati, C. & Narasimhamurti, C.C. (1978) A new microsporidian parasite, *Toxoglugea tillargi* sp. n. from an odonate, *Tholymis tillarga*. *Acta Protozoologica*, **17**, 279–283.
- Kehlhoffner, J.-L. & Dietrich, J. (1983) Synaptonemal complex and a new type of nuclear polycomplex in three higher plants: *Paeonia tenuifolia*, *Paeonia delavayi*, and *Tradescantia pallida*. *Chromosoma*, **88**, 164–170.
- Larsson, R. (1983) *Thelohania capillata* n. sp. (Microspora, Thelohaniidae) – An ultrastructural study with remarks on the taxonomy of the genus *Thelohania* Henneguy, 1892. *Archiv für Protistenkunde*, **127**, 21–46.
- Larsson, R. (1986a) Development, ultracytology and taxonomic position of *Thelohania corethrae* Schuberg & Rodriguez, 1915 (Microspora, Thelohaniidae). *Archiv für Protistenkunde*, **132**, 245–264.
- Larsson, R. (1986b) Ultrastructural investigation of two microsporidia with rod-shaped spores, with descriptions of *Cylindrospora fasciculata* sp. nov. and *Resiomeria odonatae* gen. et sp. nov. (Microspora, Thelohaniidae). *Protistologica*, **22**, 379–398.
- Narasimhamurti, C.C., Nazeer Ahamed, S. & Kalavati, C. (1980) Two new species of microsporidia from the larvae of *Tramea limbata* (Odonata: Insecta). *Proceedings of the Indian Academy of Science (Animal Science)*, **89**, 531–535.
- Romeis, B. (1968) *Mikroskopische Technik*. München & Wien: Oldenbourg Verlag, 757 pp.
- Sprague, V., Vernick, S.H. & Lloyd Jr., B.J. (1968) The fine structure of *Nosema* sp. Sprague, 1965 (Microsporida, Nosematidae) with particular reference to stages in sporogony. *Journal of Invertebrate Pathology*, **12**, 105–117.
- Vávra, J. (1984) *Norlevinea* n. g., a new genus for *Glugea daphniae* (Protozoa: Microspora), a parasite of *Daphnia longispina* (Crustacea: Phyllopoda). *Journal of Protozoology*, **31**, 508–513.
- Vetterling, J.M. & Thompson, D.E. (1972) A polychromatic stain for use in parasitology. *Stain Technology*, **47**, 164–165.
- Vinnikova, N.V. (1976) Conjugation in the ciliate *Dileptus anser*. I. Ultrastructure of micronuclei during mitosis and meiosis. *Protistologica*, **12**, 7–24.
- Weiser, J. & Žižka, Z. (1975) Stages in sporogony of *Plistonaphora debaisieuxi* Jirovec. *Acta Protozoologica*, **14**, 185–194.